Langmuir

ARTICLE

pubs.acs.org/Langmuir

Dynamics of a Disturbed Sessile Drop Measured by Atomic Force Microscopy (AFM)

Patricia M. McGuiggan,*[,†] Daniel A. Grave,[†] Jay S. Wallace,[‡] Shengfeng Cheng,[§] Andrea Prosperetti,[∥] and Mark O. Robbins[∥,⊥]

[†]Department of Materials Science and Engineering, [∥]Department of Mechanical Engineering, and [⊥]Department of Physics and Astronomy, Johns Hopkins University, Baltimore, Maryland 21218, United States

[‡]MACS Consulting, Germantown, Maryland 20874, United States

[§]Sandia National Laboratories, Albuquerque, New Mexico 87185, United States

ABSTRACT: A new method for studying the dynamics of a sessile drop by atomic force microscopy (AFM) is demonstrated. A hydrophobic microsphere (radius, $r \sim 20-30\ \mu$m) is brought into contact with a small sessile water drop resting on a polytetrafluoroethylene (PTFE) surface. When the microsphere touches the liquid surface, the meniscus rises onto it because of capillary forces. Although the microsphere volume is 6 orders of magnitude smaller than the drop, it excites the normal resonance modes of the liquid interface. The sphere is pinned at the interface, whose small (<100 nm) oscillations are readily measured with AFM. Resonance oscillation frequencies were measured for drop volumes between 5 and 200 μL. The results for the two lowest normal modes are quantitatively consistent with continuum calculations for the natural frequency of hemispherical drops with no adjustable parameters. The method may enable sensitive measurements of volume, surface tension, and viscosity of small drops.

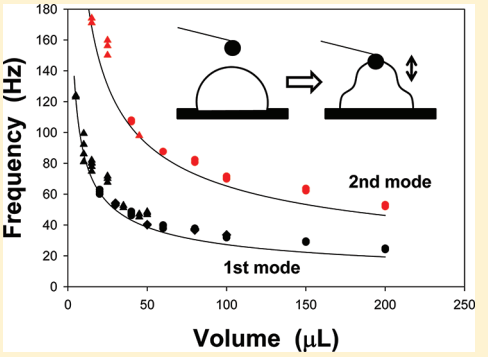

INTRODUCTION

Interfacial dynamics of fluids and, in particular, drops are important in a variety of technological processes, such as foaming, flotation, emulsification, coating, ink jet printing, microencapsulation, detergency, distillation, microelectromechanical systems (MEMS), hard disk drives, oil recovery, crystallization, and catalysis.[1−3] Because of the technological importance, the dynamic properties of fluid interfaces should be understood, at both the macro- and nanoscale. As a contribution toward this goal, we report a new method for measuring the interfacial dynamic properties of disturbed sessile drops.

Numerous experimental methods have been devised to investigate the dynamics of fluid interfaces. Experimental methods, such as the Faraday wave method,[4−6] oscillating barrier,[7] elastic ring methods,[8−10] capillary wave method,[11−14] and oscillating bubble and drop methods,[15−17] involve a variety of interface shapes, deformations, and frequency ranges. A theoretical understanding of the experimental measurements generally requires knowledge of the fluid motion and boundary conditions at the solid/fluid/air contact line.[18−20] For example, during wetting or dewetting, the contact line might be pinned or it can slip over the surface as the meniscus advances or recedes.[21]

Atomic force microscopy (AFM) is typically used to image surfaces and study the force of interaction between the AFM probe and a surface.[22,23] A few researchers have used AFM to investigate wetting properties of AFM tips, colloidal probes, nanowires, microrods, and surfaces.[24−30] In these experiments, the wetting force is typically measured at a particular immersion depth and the contact angle is calculated from models of the shape of the interface. The dynamics of the liquid interface has not been studied using AFM.

In this work, the interface of a sessile drop is suddenly perturbed by a microsphere touching the air/water interface, resulting in an immediate capillary rise onto the microsphere. Because the cantilever has such a high resonance frequency compared to the drop, the motion of the cantilever follows the motion of the interface once contact occurs. Even though the microsphere volume is 6 orders of magnitude smaller than the drop, the amplitude of the oscillation is readily measured with AFM. Sharp resonance frequencies are observed that vary with the volume of the drop. The two lowest resonance frequencies are measured as a function of the drop volume. To our knowledge, this is the first time that the two distinct modes of oscillation have been simultaneously measured for a sessile drop. A theoretical model of sessile drop vibrations quantitatively fits the data with no adjustable parameters.

EXPERIMENTAL SECTION

Soda lime glass microspheres (Polysciences, Inc., Warrington, PA) were used for the measurements. AFM measurements of the surface

Received: June 23, 2011
Revised: August 9, 2011
Published: August 17, 2011

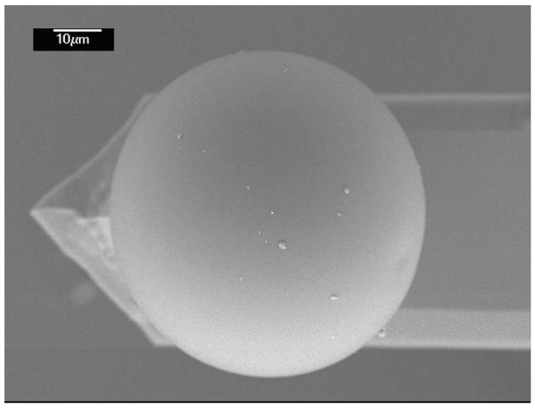

(a)

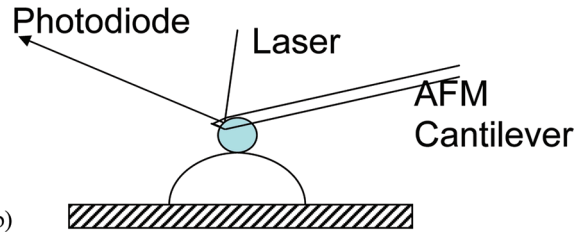

(b)

Figure 1. (a) SEM image of a glass microsphere attached to an AFM cantilever. (b) Schematic diagram of the AFM configuration just before a hydrophobic microsphere contacts a fluid droplet. Note that the diagram is not drawn to scale, as the drop radius is approximately 2 orders of magnitude larger than the radius of the microsphere.

roughness of a 4 μm^2 area of the untreated microspheres showed a root-mean-square (rms) roughness of 0.3 nm. The microspheres were washed in dilute HCl solution, rinsed in distilled water, and exposed to a UV cleaner (PSD-UV, Novascan Technologies, Inc., Ames, IA) for 10 min. A microsphere was then attached to the end of an intermittent/tapping mode AFM cantilever (Bruker Nano, Santa Barbara, CA; RTESPW cantilevers) using fast setting epoxy (Hardman, Royal Adhesives and Sealants, South Bend, IN). Figure 1a shows a scanning electron microscopy (SEM) micrograph of a glass microsphere attached to the end of an AFM cantilever. Other images showing the epoxy bond have been previously published.[31] The nominal spring constant and length of the cantilevers were 40 N/m and 125 ± 5 μm, respectively. The placement of the microsphere on the cantilever will affect the spring constant. However, the stiffness does not affect the oscillation frequency that is our focus here. Consistent results were obtained with at least three different spheres and cantilevers to check that surface roughness and stiffness did not affect oscillation frequencies.

The mounted microsphere was exposed to a vapor of methyl trichlorosilane for 2 min to make it hydrophobic. The hydrophobic coating was necessary to prevent the fluid from wetting the entire sphere and cantilever. Such complete wetting was observed when a bare sphere and cantilever were cleaned in an ultraviolet plasma cleaner prior to testing. This wetting behavior is expected, as will be shown later.

A Dimension 3100 AFM (Bruker Nano, Santa Barbara, CA) was used for the AFM measurements. The photodiode signal was independently calibrated by pressing the sphere bonded onto the AFM cantilever onto a hard silicon surface and noting the deflection of the cantilever. Because of the large difference in stiffness between the glass microsphere and the cantilever, the deformation effect of the sphere is expected to be small compared to the cantilever deflection. The deflection sensitivity of the photodiode was near 50 nm/V.

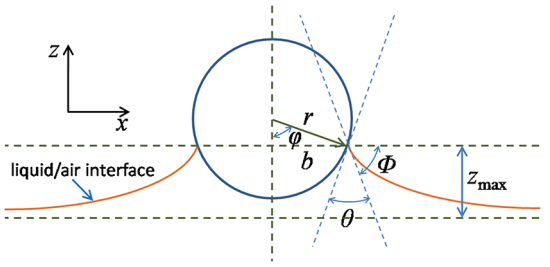

Figure 2. Schematic diagram of a sphere partially immersed in a liquid, showing the parameters used to calculate the meniscus rise. For the case of a microsphere, the meniscus height decreases gradually with the distance from the microsphere over a length scale of the order of the sphere radius.

A polytetrafluoroethylene (PTFE) surface (2 mm thick) was washed in concentrated NaOH solution, thoroughly rinsed in distilled water, and dried. A water droplet was gently placed on the PTFE surface. The microsphere on the AFM cantilever was centered over the midpoint of the droplet and slowly lowered using the stepper motor of AFM, with an average rate of approach of 2.92 μm/s. In the absence of an interaction force between the microsphere and the sessile drop, the photodiode signal was insensitive to the movement of the stepper motor in air. The stepper motor was stopped once contact between the droplet and the sphere occurred, as noted by the sudden change in the photodiode signal. During the measurement, the laser signal was focused near the center of the photodiode, where the photodiode was calibrated. The photodiode signal was directly monitored by a digital recorder (data logger), which recorded between 200 and 400 data points per second.

Deionized water with a resistivity greater than 18.2 MΩ cm (Milli-Q Synthesis A10, Millipore, MA) and a surface tension of 72 mN/m[32] was used for the droplets. The contact angle of a water drop on the PTFE surface was measured to be 95° using a goniometer. The experiments were performed at 24 ± 1 °C.

RESULTS

A diagram of the experimental configuration before contact of the microsphere with the droplet is shown in Figure 1b. Note that the figure is not drawn to scale, as the droplet radius is approximately 2 orders of magnitude larger than the microsphere radius. When the microsphere contacts the air/water interface, the meniscus will climb onto it. For a macroscopic solid, the meniscus rise onto a solid surface is the same order of magnitude as the capillary length, $c = (\gamma_{lv}/\Delta\rho g)^{1/2}$, where γ_{lv} is the liquid/vapor surface tension, $\Delta\rho$ is the density difference between the liquid and the vapor, and g is the acceleration due to gravity.[33] For water, c = 2.7 mm. However, when the probe radius $r \ll c$, the meniscus rise height z scales with the microsphere radius and depends upon the contact angle of the liquid with the microsphere. To the first order in r/c, the entire liquid/vapor interface is given by the equation[34]

$$z(x) = b \sin \Phi[\ln 2x - \ln(x^2 - \sqrt{x^2 - b^2 \sin^2 \Phi}) + K_0(x/c)] \quad (1)$$

where x is the horizontal distance from the central axis of the microsphere, Φ is the angle between the tangent of the liquid/air interface at the microsphere surface and the horizontal direction, b is the radius of the spanning circle of the contact line on the microsphere surface, and $K_0(x/c)$ is the modified Bessel function of order zero. This is the general axisymmetric solution for the interface shape and can be applied to any axisymmetric solid by

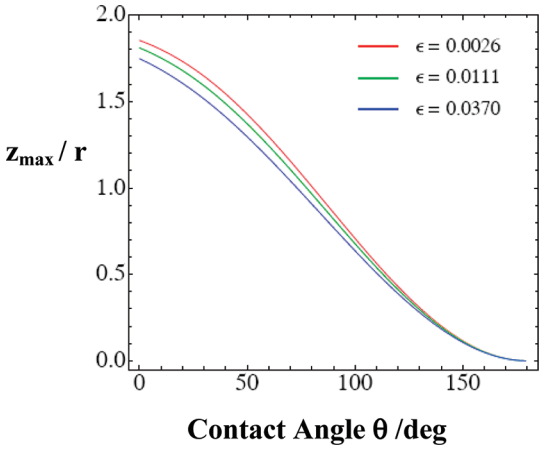

Figure 3. Maximum meniscus rise height above the undeformed fluid interface, z_{max}, scaled by the sphere radius r. The plots are shown as a function of the contact angle for various values of the dimensionless parameter $\varepsilon = r/c$, where $c = (\gamma_{lv}/\Delta\rho g)^{1/2}$.

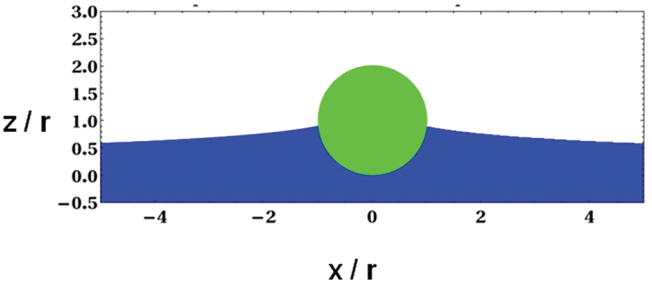

Figure 4. Illustration of the wetting of the microsphere. The meniscus height, z, and horizontal distance, x, are scaled by the radius of the sphere r. Note that $z/r = 0$ corresponds to the height of the undeformed fluid interface.

properly choosing the boundary conditions b and Φ.[34−36] Applying these conditions to a spherical geometry, one finds that the maximum rise height of the meniscus above the undeformed fluid interface is given by[34,37,38]

$$z_{max} = x \sin\Phi\left[\ln\frac{4c}{x(1+\cos\Phi)} - \gamma_E\right] = r\sin\varphi\sin(\varphi+\theta)\left[\ln\frac{4}{\varepsilon\sin\varphi(1-\cos(\varphi+\theta))} - \gamma_E\right] \quad (2)$$

where γ_E is Euler's constant ($\gamma_E = 0.577\,215...$), φ is the spanning angle of the contact line on the microsphere surface, θ is the contact angle of the liquid against the microsphere, and $\varepsilon = r/c$ is a dimensionless number (ε^2 = Bond number). A schematic diagram of the meniscus rise onto the microsphere and the geometric parameters used in the calculations is shown in Figure 2. As noted above, eq 1 is a general axisymmetric solution for the interface shape. Changing from sphere to rod to cone only affects the relation between the boundary condition embodied by the angle Φ at a given radius b.[34−36]

Figure 3 shows the maximum meniscus rise above the undeformed fluid interface, z_{max}, calculated from eq 2, scaled by the microsphere radius. The maximum meniscus rise will occur at the three-phase line, where the liquid is in contact with the microsphere. The curves in Figure 3 represent the maximum meniscus rise for various values of the dimensionless parameter $\varepsilon = r/c$. For the measurements reported, the microsphere was hydrophobic (advancing contact angle $\theta_a \approx 90$), with a typical radius $20 < r < 35\ \mu$m and $\varepsilon \approx 0.01$. For $\varepsilon = 0.01$ and a contact angle of 85°, Figure 3 shows that the meniscus is predicted to rise to near the middle of the microsphere ($0.9r$). This meniscus rise is shown schematically in Figure 4, where the rise height and distance are scaled by the radius of the sphere. The meniscus height in eq 2 decays slowly from the edge of the microsphere, as shown by Figure 4, where the meniscus rise z is approximately $0.6r$ at a distance 4 times the microsphere radius. The meniscus height has fallen to $1/e$ of z_{max} at a distance 19 times the microsphere radius from the central axis. Note that, even though the microsphere is hydrophobic, the meniscus rises onto it.

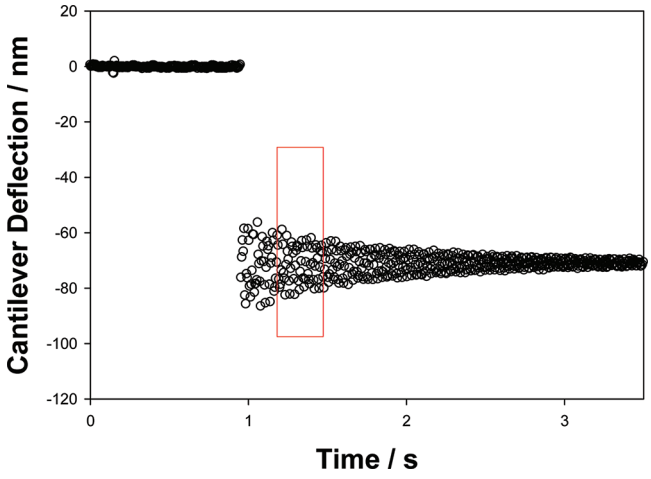

Figure 5. Measured cantilever deflection as a function of time. The microsphere is brought into contact with a 100 μL water droplet at approximately 1 s. The data within the rectangle are expanded in Figure 6.

Measurements of the force of the capillary rise were performed using AFM. For the AFM measurements, it is important that the meniscus does not rise to touch the epoxy layer attaching the sphere to the cantilever,[31] where the geometry and surface properties change. To avoid this condition, it is required that $z_{max} < 1.7r$, and according to Figure 3, the contact angle of the meniscus next to the sphere should be $\geq 40°$; this condition is fulfilled for hydrophobic microspheres.

Experimentally, the meniscus rise on the microsphere is observed as an abrupt change in the cantilever deflection, as measured by the AFM photodiode signal. Once contact between the microsphere and the droplet occurs, the AFM motor is stopped. Figure 5 shows the measured cantilever deflection as a function of time as a microsphere ($r = 20\ \mu$m) is brought into contact with a 100 μL water droplet on PTFE. Minimal deflection is seen as the sphere is brought toward the interface. Once contact occurs, the meniscus exerts a force on the microsphere, which pulls it toward the droplet (at time $t \approx 1$ s). Because the cantilever is relatively stiff (spring constant $k \sim 40$ N/m), the cantilever deflection is only 72 nm. The predicted maximum meniscus rise above the undeformed droplet interface, z_{max}, according to eq 2, is approximately 18 μm for a contact angle near 90°. Because the cantilever only deflects 72 nm on contact, while the meniscus rises 18 μm onto the microsphere, the bottom of the microsphere can be taken

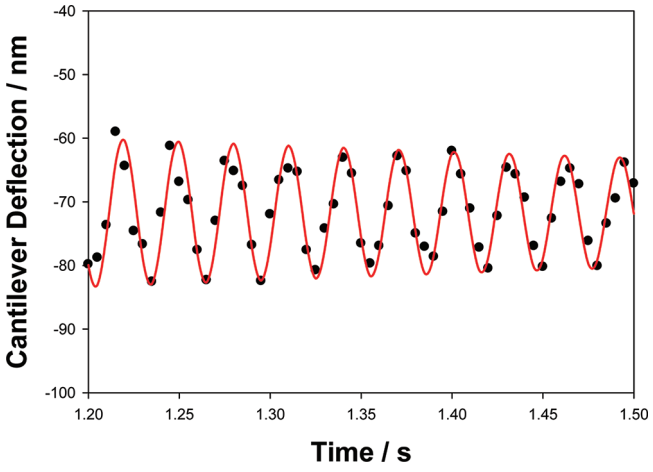

Figure 6. Expanded graph of the highlighted region of data shown in Figure 5. The solid line is a fit to the data using a five-parameter damped sine wave equation given by eq 4. Small deviations from the fit reflect both noise and the contribution of other normal modes.

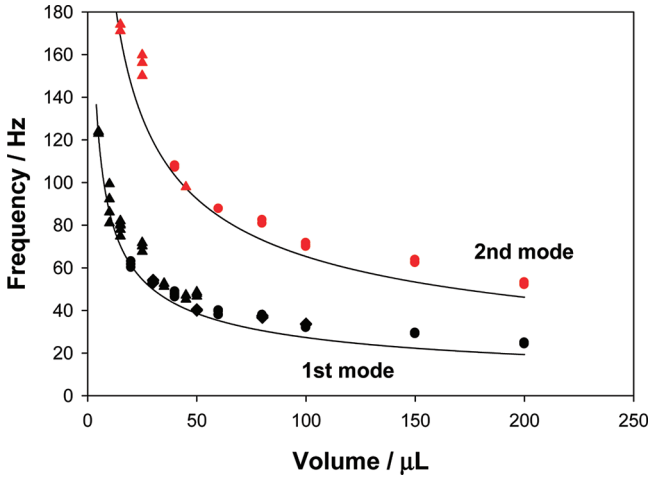

Figure 7. First and second resonance mode oscillation frequency as a function of the water drop volume. The contact angle of the sessile drop on the PTFE surface was 95°. The solid circles, squares, and triangles represent data from three experiments using a different sphere and cantilever for each experiment. The solid curves represent the expected resonance frequency for a water drop on a flat surface with a contact angle of 90°, as given by eqs 5 and 6. Note that no fitting parameters are used in the equation. The equation assumes that gravity can be neglected, which is valid when the radius of the drop is less than the capillary length ($V < 60\ \mu$L).

to be even with the undeformed droplet interface, as shown in Figure 4.

The meniscus force, F, found by multiplying the cantilever deflection by the cantilever spring constant, depends upon the meniscus height and the position of the meniscus on the microsphere. The meniscus force for a microsphere of radius r for the geometry shown in Figure 2 is given by[34,35,38−40]

$$F = \pi\Delta\rho g r^3\left[2\varepsilon^{-2}\sin\varphi\sin(\varphi + \theta) + \frac{z_{max}}{r}\sin^2\varphi - \frac{1}{3}(2 - 3\cos\varphi + \cos^3\varphi)\right] \quad (3)$$

All parameters have been previously defined or are defined in Figure 2. The first term in the brackets represents the contribution from the liquid/vapor surface tension, and the second term represents the contribution from the excess pressure because of the meniscus rise. The third term is the buoyancy force resulting from partial immersion of the microsphere in the liquid. For micrometer-sized materials, this buoyancy force is negligible.

Immediately after the initial rise of the meniscus, the microsphere oscillates about a fixed average position while partially immersed in the liquid. Figure 6 shows an expanded section of the data outlined in Figure 5. Because of the constant average deflection, we can assume that the microsphere/water contact line is pinned and the measured oscillation reflects the motion of the sessile drop interface. For this experiment, the maximum peak to peak oscillation amplitude was 40 nm and the amplitude decreased to the background vibrations within 2 s. The solid line in Figure 6 is a five-parameter damped sine wave fit to the data given by

$$y = y_0 + A\exp(-t/D)\sin(C + 2\pi Bt) \quad (4)$$

where y is the cantilever deflection, y_0 is the average cantilever deflection, A is the oscillation amplitude, B is the frequency, C is the phase offset, t is the time, and D is the damping time. For this particular data set (100 μL water drop), B = 33 Hz and D = 0.9 s. Further experiments showed that both the oscillation frequency and the damping depended upon the volume of the drop.

Figure 7 shows results for the measured oscillation frequency as a function of the droplet volume. For each measurement, the data were analyzed by finding the position of peaks in the Fourier power spectrum. Because the highest sampling rate was 400 Hz, the highest detectable frequency was 200 Hz. In most experiments, two resonance modes were found, and their frequencies are shown in Figure 7. The amplitude of the second mode was typically 3−8 times smaller than that of the first mode. In all cases, the same PTFE surface was used as the substrate and water was used as the liquid. The circles, squares, and triangles represent the data obtained for three experiments using a different microsphere and AFM cantilever for each experiment. The data show an increase in the oscillation frequency as the drop volume decreases. The measured frequency is what would be expected if the entire drop oscillated, as will be discussed later.

The solid curves in Figure 7 show the first and second normal mode oscillation frequency predicted theoretically as a function of the drop volume.[41] In this theory, an inviscid hemispherical drop (θ = 90°) is assumed to be resting on a flat surface.[41] In addition, it is assumed that the oscillation amplitude is small and that the droplet is pinned at the three-phase line (PTFE/air/fluid interface). Previous measurements of the small-amplitude vibration of vibrated sessile drops and the evaporation of drops on PTFE have found that the contact line is pinned.[42,43]

The theoretical curve is calculated by finding the values of $\tilde{\omega}_k$ that satisfy[41]

$$f(\tilde{\omega}_k) \equiv \sum_{\ell=1}^{\infty}\frac{\ell(4\ell + 1)}{\tilde{\omega}_k^2 - 4\ell(2\ell - 1)(\ell + 1)}\left[\frac{(2\ell - 1)!!}{2^\ell\ell!}\right]^2 = 0 \quad (5)$$

where $\tilde{\omega}_k{}^2 = (\rho a^3/\gamma_{lv})\omega_k{}^2$ and a is the radius of the contact line of the drop with the substrate surface. Because a hemispherical drop is assumed, $a = r = ((3/2\pi)V)^{1/3}$. For the first two resonance

modes, a numerical solution of eq 5 (with the infinite summation truncated at ℓ = 1000), gives $\tilde{\omega}_k$ = 4.417 13 and 10.5706. The resonance frequency is then calculated from

$$f(k) = \omega_k = \frac{1}{2\pi}\sqrt{\frac{\gamma_{lv}\tilde{\omega}_k^2}{\rho a^3}} = \sqrt{\frac{\gamma_{lv}\tilde{\omega}_k^2}{6\pi\rho V}} \quad (6)$$

Note that all of the parameters in eq 6 are either known quantities (V, ρ, and γ_{sl}) or are directly calculated. There are no adjustable fitting parameters in the equation.

For small volumes (V < 60 μL), Figure 7 shows that the theoretical prediction for the first two oscillation modes quantitatively fits the data. However, at larger volumes (V > 60 μL), the theory underestimates the measured frequencies by 20−30%.

DISCUSSION

The measurements show that AFM can be used to investigate dynamic properties of millimeter-sized sessile drops. The contact of a microsphere (attached to an AFM cantilever) with a sessile drop leads to a rapid rise of the meniscus onto the microsphere. This causes a nanometer scale oscillation of the entire drop, even though the drop volume is approximately 6 orders of magnitude larger than the microsphere volume.

The measured oscillation is not due to the resonance of the cantilever, which, in air and without the attached microsphere, was near 280 kHz. With the attached microsphere, the resonance frequency in air decreased to near 25 kHz. For a mass, m, on a spring with the surface tension (restoring force) of the liquid as its spring constant, the frequency is expected to be of the order of

$$f \approx \frac{1}{2\pi}\sqrt{\frac{\gamma_{lv}}{m}} \approx 175 \text{ kHz} \quad (7)$$

where m is the mass of the microsphere. This frequency is approximately 4 orders of magnitude larger than that measured in the experiments, indicating that the "effective mass" of the system must be much larger than the mass of the microsphere. Rearranging eq 7 and substituting the frequency measured (30 Hz) shows that the "effective mass" in eq 7 is approximately 2 mg, corresponding to a water volume of about 2 μL. Although this is more than an order of magnitude smaller than the drop volume, it indicates that much of the water is contributing to the "effective mass". Also, because buoyancy is extremely small with these small spheres, the oscillations are not expected to be due to buoyancy.

Because the natural frequency of the combined cantilever and microsphere is so high, they can easily follow the movement of the meniscus. Measurement of their motion with AFM allows for the interface motion to be tracked. The cantilever and the surface tension of the interface can be considered to be two springs in series. The spring constant of the system is given by the spring constant of the weakest spring, the surface tension of the interface. This is shown mathematically as $1/k_{system} = 1/k_{cantilever} + 1/\gamma_{lv} \approx 1/\gamma_{lv}$ because $k_{cantilever} \approx 40$ N/m and $\gamma_{lv} \approx 72$ mN/m.

For small volumes (V < 60 μL), the theoretical prediction for the first and second oscillation modes quantitatively fits the data. However, at larger volumes (V > 60 μL), the theory underestimates the measured frequencies. The theory assumes that the drop shape is hemispherical. The drop profile can be determined by the Young−Laplace equation for given values of the capillary length c, drop radius R, and contact angle of the droplet on the surface, θ_s. If $R \ll c$, the gravitational effects are negligible and the drop assumes a hemispherical shape to minimize the surface energy. When $R \sim c$, the drop becomes flattened because of the effects of gravity.[44,45] For the measurements reported, $R \sim c$ for V = 60 μL. Optical measurements of the height of sessile drops on a hydrophobic paraffin surface (θ_s = 107°) are shown in Figure 8. The solid curve is the theoretical prediction for the height of a spherical drop with a contact angle of 107°. The measured drop height increases with drop volume until the drop volume exceeds 60 μL. At larger volumes, even though the drop volume increases, the drop height remains nearly constant. The maximum measured drop height was found to be 3.2 mm, which is near the capillary length of 2.7 mm. Because the theory for sessile drop oscillations discussed above assumes a hemispherical drop shape (θ_s = 90°), it is reasonable to expect a small discrepancy between the theory and the data at larger volumes, as was observed. A further difference between theory and experiment is expected because the contact angle of water on PTFE was 95° instead of 90°. A similar theory for drop resonance supported on a spherical cap (as opposed to a flat surface) has been shown to be applicable for contact angles greater than 90°, although different eigenvalues must be calculated for each contact angle.[46,47]

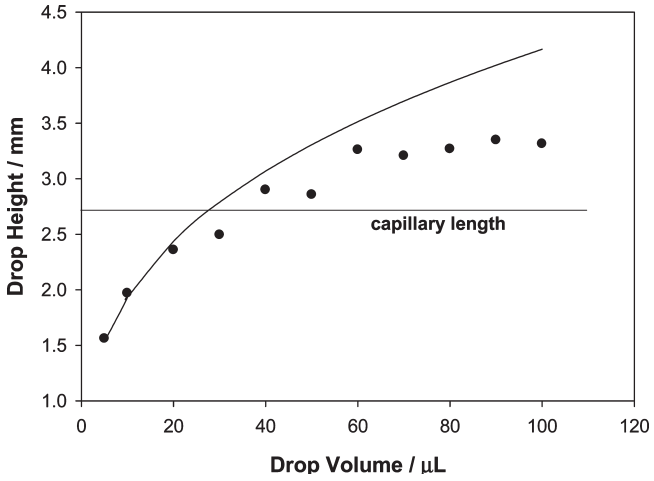

Figure 8. Measured drop height of a sessile drop of water placed on a paraffin surface. The contact angle was measured to be 107° ± 2°. The solid line is the predicted drop height for a hemispherical drop having a contact angle of 107°. The data rise less rapidly for drop heights exceeding the capillary length of 2.7 mm.

Fourier transform analysis of the data show that two different modes of oscillation are present. The ability to detect a resonance mode by Fourier transform depends upon the data collection rate, and because the sampling rate was 200−400 points/s, we were limited to detecting resonance frequencies less than 200 Hz. It is possible that higher normal modes are also excited and underdamped, but the data collection rate must be increased before they can be observed.

Note that the calculation of droplet resonance frequency in eq 6 is independent of the size and chemistry of the probe, i.e., the contact angle of the liquid with the probe. This has been confirmed by preliminary experiments. Oscillations have been observed for the wetting of both hydrophilic and hydrophobic microrods (r = 50 μm),[24] as well as hydrophobic microspheres.

However, oscillations have not been observed during the wetting of nanowires (r < 200 nm), presumably because of the relatively small perturbation.

The oscillation frequency of the droplet is determined by the droplet volume, fluid density, surface tension, contact angle of the droplet on the substrate, and mode of oscillation. Because the first three are generally known, it should be possible to obtain the contact angle of a sessile drop on a solid surface by measuring the oscillation frequency and fitting to theoretical predictions. Unfortunately, no theories exist that properly account for oscillation frequencies for contact angles other than 90°. We are currently investigating other surfaces, liquids, surface tensions, and contact angles to better test the current theories and limits of the measurement.

CONCLUSION

A new method for studying the dynamics of a sessile drop by AFM is demonstrated. The droplet interface was perturbed by the contact of a microsphere with the liquid and immediate rise of the meniscus onto the microsphere. Fourier transform analysis of the data shows that two different modes of oscillation of the droplet are present. To our knowledge, this is the first time that two distinct modes of oscillation have been simultaneously measured for a sessile drop. The measured frequencies corresponded to the small amplitude vibration of the entire drop and were fitted to theories for resonance vibrations of a sessile droplet with no adjustable parameters. This method can be used to study droplet dynamics or to determine the volume, surface tension of the fluid, or contact angle of the sessile drop on the surface.

AUTHOR INFORMATION

Corresponding Author

*E-mail: patricia.mcguiggan@jhu.edu.

DISCLOSURE

Disclosure: Any opinions, findings, and conclusions or recommendations expressed in this paper are those of the authors and do not necessarily reflect the views of the National Science Foundation (NSF).

ACKNOWLEDGMENT

Patricia M. McGuiggan thanks Lee White and Derek Chan for helpful discussions. This material is based on work supported by the 3M Nontenured Faculty Grant and the National Science Foundation (NSF) under Grant CMMI-0709187.

REFERENCES

(1) Miller, C. A.; Neogi, P. *Interfacial Phenomena*; Marcel Dekker, Inc.: New York, 1985; Vol. 17.

(2) Pashley, R. M.; Karaman, M. E. *Applied Colloid and Surface Chemistry*; John Wiley and Sons, Ltd.: New York, 2004.

(3) *Wettability*; Berg, J. C., Ed.; Marcel Dekker, Inc.: New York, 1993.

(4) Douady, S. Experimental study of the Faraday instability. *J. Fluid Mech.* **1990**, *221*, 383–409.

(5) Ben-David, O.; Assaf, M.; Fineberg, J.; Meerson, B. Experimental study of parametric autoresonance in Faraday waves. *Phys. Rev. Lett.* **2006**, *96* (15), No. 154503.

(6) Perlin, M.; Schultz, W. W. Capillary effects on surface waves. *Annu. Rev. Fluid Mech.* **2000**, *32*, 241–274.

(7) Lucassen, J.; Vandente, M. Longitudinal waves on viscoelastic surfaces. *J. Colloid Interface Sci.* **1972**, *41* (3), 491–498.

(8) Loglio, G.; Tesei, U.; Cini, R. Spectral data of surface viscoelastic modulus acquired via digital Fourier transformation. *J. Colloid Interface Sci.* **1979**, *71* (2), 316–320.

(9) Loglio, G.; Tesei, U.; Cini, R. Viscoelastic dilatation processes of fluid fluid interfaces—Time-domain representation. *Colloid Polym. Sci.* **1986**, *264* (8), 712–718.

(10) Miller, R.; Loglio, G.; Tesei, U.; Schano, K. H. Surface relaxations as a tool for studying dynamic interfacial behavior. *Adv. Colloid Interface Sci.* **1991**, *37* (1−2), 73–96.

(11) Noskov, B. A.; Alexandrov, D. A.; Miller, R. Dynamic surface elasticity of micellar and nonmicellar solutions of dodecyldimethyl phosphine oxide. Longitudinal wave study. *J. Colloid Interface Sci.* **1999**, *219* (2), 250–259.

(12) Lemaire, C.; Langevin, D. Longitudinal surface waves at liquid interfaces—Measurement of monolayer viscoelasticity. *Colloids Surf.* **1992**, *65* (2−3), 101–112.

(13) Langevin, D. Capillary-wave techniques for the measurement of surface tension and surface viscoelasticity. *Colloids Surf.* **1990**, *43* (2−4), 121–131.

(14) Behroozi, F.; Lambert, B.; Buhrow, B. Direct measurement of the attenuation of capillary waves by laser interferometry: Noncontact determination of viscosity. *Appl. Phys. Lett.* **2001**, *78* (16), 2399–2401.

(15) Chang, C. H.; Coltharp, K. A.; Park, S. Y.; Franses, E. I. Surface tension measurements with the pulsating bubble method. *Colloids Surf., A* **1996**, *114*, 185–197.

(16) Chang, C. H.; Franses, E. I. An analysis of the factors affecting dynamic tension measurements with the pulsating bubble surfactometer. *J. Colloid Interface Sci.* **1994**, *164* (1), 107–113.

(17) Wantke, K. D.; Lunkenheimer, K.; Hempt, C. Calculation of the elasticity of fluid boundary phases with the oscillating bubble method. *J. Colloid Interface Sci.* **1993**, *159* (1), 28–36.

(18) Thompson, P. A.; Brinckerhoff, W. B.; Robbins, M. O. Microscopic studies of static and dynamic contact angles. *J. Adhes. Sci. Technol.* **1993**, *7* (6), 535–554.

(19) Jiang, L.; Perlin, M.; Schultz, W. W. Contact-line dynamics and damping for oscillating free surface flows. *Phys. Fluids* **2004**, *16* (3), 748–758.

(20) Obrien, S. B. G. The meniscus near a small sphere and its relationship to line pinning of contact lines. *J. Colloid Interface Sci.* **1996**, *183* (1), 51–56.

(21) Nadkarni, G. D.; Garoff, S. An investigation of microscopic aspects of contact-angle hysteresis—Pinning of the contact line on a single defect. *Europhys. Lett.* **1992**, *20* (6), 523–528.

(22) Eaton, P.; West, P. *Atomic Force Microscopy*; Oxford University Press: Oxford, U.K., 2010.

(23) *Scanning Probe Microscopy and Spectroscopy: Theory, Techniques, and Applications*, 2nd ed.; John Wiley and Sons, Ltd.: New York, 2001.

(24) McGuiggan, P. M.; Wallace, J. S. Maximum force technique for the measurement of the surface tension of a small droplet by AFM. *J. Adhes.* **2006**, *82* (10), 997–1011.

(25) Ecke, S.; Preuss, M.; Butt, H. J. Microsphere tensiometry to measure advancing and receding contact angles on individual particles. *J. Adhes. Sci. Technol.* **1999**, *13* (10), 1181–1191.

(26) Tao, Z. H.; Bhushan, B. Wetting properties of AFM probes by means of contact angle measurement. *J. Phys. D: Appl. Phys.* **2006**, *39* (17), 3858–3862.

(27) Nguyen, A. V.; Nalaskowski, J.; Miller, J. D. The dynamic nature of contact angles as measured by atomic force microscopy. *J. Colloid Interface Sci.* **2003**, *262* (1), 303–306.

(28) Barber, A. H.; Cohen, S. R.; Wagner, H. D. Static and dynamic wetting measurements of single carbon nanotubes. *Phys. Rev. Lett.* **2004**, *92* (18), No. 186103.

(29) Yazdanpanah, M. M.; Hosseini, M.; Pabba, S.; Berry, S. M.; Dobrokhotov, V. V.; Safir, A.; Keynton, R. S.; Cohn, R. W. Micro-Wilhelmy and related liquid property measurements using constant-diameter nanoneedle-tipped atomic force microscope probes. *Langmuir* **2008**, *24* (23), 13753–13764.

(30) Uddin, M. H.; Tan, S. Y.; Dagastine, R. R. Novel characterization of microdrops and microbubbles in emulsions and foams using atomic force microscopy. *Langmuir* **2011**, *27* (6), 2536–2544.
(31) McGuiggan, P. M.; Zhang, J.; Hsu, S. M. Comparison of friction measurements using the atomic force microscope and the surface forces apparatus: The issue of scale. *Tribol. Lett.* **2001**, *10* (4), 217–223.
(32) *Handbook of Chemistry and Physics*, 58th ed.; CRC Press (Taylor and Francis Group): Boca Raton, FL, 1978.
(33) Kayser, R. F.; Schmidt, J. W.; Moldover, M. R. Wetting layers and dispersion forces for a fluid in contact with a vertical wall. *Phys. Rev. Lett.* **1985**, *54* (7), 707–710.
(34) James, D. F. Meniscus on outside of a small circular cylinder. *J. Fluid Mech.* **1974**, *63* (May 15), 657–664.
(35) Scheludko, A. D.; Nikolov, A. D. Measurement of surface-tension by pulling a sphere from a liquid. *Colloid Polym. Sci.* **1975**, *253* (5), 396–403.
(36) Huh, C.; Scriven, L. E. Shapes of axisymmetric fluid interfaces of unbounded extent. *J. Colloid Interface Sci.* **1969**, *30* (3), 323–337.
(37) Lyons, C. J.; Elbing, E.; Wilson, I. R. The rod-in-free surface technique for surface-tension measurement using small rods. *J. Colloid Interface Sci.* **1984**, *102* (1), 292–294.
(38) Lo, L. L. The meniscus on a needle—A lesson in matching. *J. Fluid Mech.* **1983**, *132*, 65–78.
(39) Padday, J. F.; Pitt, A. R.; Pashley, R. M. Menisci at a free liquid surface—Surface tension from maximum pull on a rod. *J. Chem. Soc., Faraday Trans. 1* **1975**, *71*, 1919–1931.
(40) Gunde, R.; Hartland, S.; Mader, R. Sphere tensiometry—A new approach to simultaneous and independent determination of surface tension and contact angle. *J. Colloid Interface Sci.* **1995**, *176* (1), 17–30.
(41) Lyubimov, D. V.; Lyubimova, T. P.; Shklyaev, S. V. Behavior of a drop on an oscillating solid plate. *Phys. Fluids* **2006**, *18* (1), 012101-1–012101-11.
(42) Noblin, X.; Buguin, A.; Brochard-Wyart, F. Vibrated sessile drops: Transition between pinned and mobile contact line oscillations. *Eur. Phys. J. E: Soft Matter Biol. Phys.* **2004**, *14* (4), 395–404.
(43) Shi, L. X.; Shen, P.; Zhang, D.; Lin, Q. L.; Jiang, Q. C. Wetting and evaporation behaviors of water−ethanol sessile drops on PTFE surfaces. *Surf. Interface Anal.* **2009**, *41* (12−13), 951–955.
(44) Padday, J. F. Heights of sessile drops and meniscus properties. *Nature* **1963**, *198* (487), 378–379.
(45) Padday, J. F. Sessile drop profiles—Comparison with Searles equation for drop height. *J. Colloid Interface Sci.* **1974**, *48* (1), 170–171.
(46) Strani, M.; Sabetta, F. Free vibrations of a drop in partial contact with a solid support. *J. Fluid Mech.* **1984**, *141* (April), 233–247.
(47) McHale, G.; Elliott, S. J.; Newton, M. I.; Herbertson, D. L.; Esmer, K. Levitation-free vibrated droplets: Resonant oscillations of liquid marbles. *Langmuir* **2009**, *25* (1), 529–533.